

KW

Met 0 11 Technical Note No. 232

METEOROLOGICAL OFFICE

148258

-4 JUN 1986 ✓

LIBRARY

Geometric models of
balanced flow

by G.J. Shutts, S. Chynoweth
and M.J.P. Cullen

May 1986

N.B. This paper has not been published. Permission to quote from it must be obtained from the Assistant Director of the Forecasting Research Branch of the Meteorological Office.

1) An outline of the method

The principal idea behind the geometric approach to modelling atmospheric (or oceanic) flows is that of constructing a sequence of convectively and inertially stable equilibrium states which represent flow evolution on a time scale greater than f^{-1} . It provides a rigorously proven methodology for carrying the philosophy of integrating filtered meteorological equations of motion (Eliassen, 1948) to its logical conclusion without using coordinate transformations. The method allows one to integrate Eliassen's quasi-static equations in their inviscid form and avoids the need to artificially smooth fields when discontinuities appear. The theory behind the method is explained in Cullen and Purser (1984). Here we provide an intuitive, physical approach to the geometric model and its applications.

Consider firstly, a one-dimensional hydrostatic column atmosphere composed of five isentropic fluid blobs of equal mass (Fig. 1). Then it is obvious that the concept of stability coupled with mass (or area in this case) conservation fully determine the equilibrium configuration with potential temperature, θ increasing with height. Suppose now that the potential temperature of each element (θ_i , $i=1,5$) is governed by a Lagrangian evolution equation of the form:

$$\frac{d\theta_i}{dt} = F_i$$

where F_i is a forcing function representing for instance radiative heating or cooling. Then the element configuration will change discontinuously when the monotonicity of θ is violated at any instant. We could for instance develop a one-dimensional radiative-convective equilibrium model

(eg. Manabe and Wetherald, 1967) where convective adjustment was explicit. The release of latent heat would require us to compute the change in mixing ratio as an element jumps. Notice that the new equilibrium configuration after convective jumps has a lower potential energy implying the release of a well-defined amount of kinetic energy.

Less obvious is the one-dimensional, barotropic model of geostrophic flow. (Fig. 2). The well-known condition for hydrodynamic stability that the absolute vorticity must be positive translates into the monotonicity of the absolute momentum $M = V_g + fx$ and elements must be ordered accordingly. This is a special case of the inertial stability condition for a circular vortex where the gradient wind angular momentum is the relevant quantity. As in the vertical column example, stabilization could involve jumps in element position though it is difficult to imagine corresponding physical processes which could lead to such inertial destabilization in the barotropic case.

By combining these two monotonicity conditions it can be shown that knowledge of each element's mass, absolute momentum and potential temperature is sufficient to uniquely determine the geometrical configuration of elements at equilibrium (mass and area are interchangeable in the incompressible case) ie. given N elements with:

$$\text{area } A_i \text{ such that } \sum_{i=1}^N A_i = \text{domain area}$$

absolute momentum M_i

and potential temperature θ_i ,

a unique configuration exists with each element taking on a convex

polygonal shape. Interfaces between elements are required (consistent with balance) to satisfy Margules formula:

$$\frac{dz}{dx} = \frac{-f\theta_0[M]}{g[\theta]} = \text{slope of the interface}$$

where $[\]$ denotes the difference across the interface and θ_0 is a constant reference potential temperature. This condition is automatically enforced by constructing the piecewise linear modified pressure $P(x,z) = \phi + 1/2 f^2 x^2$ (ϕ is the geopotential) since it can be shown that

$$fM = \frac{\partial P}{\partial x} \quad \text{and} \quad \frac{g\theta}{\theta_0} = \frac{\partial P}{\partial z}$$

The monotonicity conditions then imply that $P(x,z)$ is a convex function and this constraint for piecewise constant M and θ allows us to write:

$$P(x,z) = \max_{1 \leq j \leq N} \{ xM_j + z\theta_j + S_j \} = \max(P_j) \quad (1)$$

(P_j defines the modified pressure plane of the j th element).

Each element can be associated with a plane whose height above the x,z plane at any point corresponds to the modified pressure at the point. The intersection of these planes defines a piecewise-linear solution $P(x,z)$. The constructive algorithm requires the determination of the set of S_j values in eq. (1) such that the element areas are correct - a process that must be carried out iteratively. (Note: the region of the (x,z) plane occupied by element i corresponds to the set of (x,z) values for which

$$P_i > P_j \quad j = 1, N \\ j \neq i$$

In a time integration, we begin with a set of values A_j , M_j , θ_j and S_j . If the domain boundary is rigid and time-independent then we may regard S_j as a function of A_i , M_i and θ_i , $i=1,N$. In the classical frontogenesis problem where a pure barotropic deformation field is imposed:

$$\frac{dM_i}{dt} = -\alpha M_i \text{ and } \frac{dA_i}{dt} = -\alpha A_i$$

where α is the deformation rate. Therefore, at any future time, A_i , M_i and θ_i are known and the solution can be found by determining S_j . It turns out to be necessary to use a time-stepping approach since the iterative procedure requires a good guess for S_j .

2) Simple physical applications

Consider a simple three-element model of frontogenesis by deformation (Fig. 3a,b). The interface boundaries rotate as $[M]$ decreases in proportion to the total deformation. The two interfaces collide at the lower boundary and force warm air initially in contact with the surface upwards. The creation of a new interface corresponds to the formation and intrusion of a frontal discontinuity. The separation of the warm air from the surface is a type of occlusion process. (see Cullen, 1983 for a more detailed account).

The simple column convection model (Fig. 1) can be re-examined for the two-dimensional case. Consider a 100 element representation of an atmosphere at rest (Fig. 4a). Elements are rectangular and arranged horizontally in isentropic layers and vertically in constant M columns. A certain quantity of heat is now injected into element 30. Fig. (4b) gives the new equilibrium configuration with the convected element taking on a lens shape as it squeezes between two isentropic layers. Since elements in the vicinity of the convection move horizontally whilst conserving M , they

generate a geostrophically balanced wind (v_g) into the picture. An anticyclonic shear develops around the lens and cyclonic shear about the original position of element 30. Although this is consistent with the classical thermal forcing response of quasi-geostrophic theory it would be unwise to adopt vortex stretching arguments here since element 30 has detached itself from its initial neighbouring elements. In fact, the boundary between elements 29 and 31 after convection represents an internal discontinuity in M (this would be more obvious at higher resolution but with heat going in to the same area of physical space).

Starting from the same initial data as represented by Fig. (4a), experiments have been carried out to mimic a sea-breeze effect. Heat is injected into elements adjacent to the left-hand half of the lower boundary (the land) by an amount proportional to the area of contact of each element with the boundary. A sequence of geostrophic and hydrostatically balanced states ensues dependent on the total amount of heat which has passed through the lower boundary. Fig. 5 show such a state when a well-developed sea-breeze front has formed. Elements 21-29 inclusive were merged with elements 1-9 when their potential temperatures became equal (ie. the onset of a well-mixed convective boundary layer). It is not, however, necessary to do this and the model is capable of performing its own convective overturning as alternate elements lift off the 'land' then become cooler than elements which are receiving heat and so sink back again. Elements 30-40 have subsided over the 'sea' and elements 11-17, initially over the sea, have moved inland at the surface. Geostrophic wind velocities (v_g) are easily calculated from the M value of an element and its centroid position. Elements which have moved inland develop an alongshore wind into the picture in agreement with observation.

The unique arrangement of elements in the dry cases considered so far cannot hold in general if elements are moist and able to release latent heat energy. For instance, in the one-dimensional model of Fig. 1 the lowest element might be saturated and have an equivalent potential temperature greater than the other elements. Then another stable arrangement can be achieved by moving the moist element to the top and the others down. For most cases where semi-geostrophic theory is relevant this is unlikely to cause problems and a physically plausible sequence of moist equilibrium states can be constructed.

A pseudo-moist process has been used to demonstrate the potential of the model to represent slantwise convection in frontal zones. This simply involves taking one element of the model and progressively increasing its potential temperature simulating the effect of latent heat release. The initial 'frontal' data is given in Fig. 6a. Note that elements defining isentropic layers are bounded laterally by vertical interfaces whereas constant M layers involve elements separated by horizontal interfaces. Element 28 is now given a 40°K increase in θ in steps of 4°K. The new equilibrium configuration is given in Fig. 6b and shows a slantwise 'jump' to a level near the tropopause. In principle, it is possible to compute the total (kinetic and potential) energy before and after such a jump and thereby calculate (for a real moist process) the SCAPE. (Slantwise Convective Available Potential Energy). Note that this method would be more general than the usual parcel method (eg. Emanuel (1983)) since an environmental adjustment would also be accounted for.

Realistic 2-D frontogenesis models are currently being developed which incorporate a moist boundary layer. Surface friction acts to change the M value of elements in contact with the surface through their implied v_g .

Boundary layer elements move toward the surface cold front and then perform slantwise jumps up the frontal (M) surface. A simple rectilinear hurricane (or squall line) model is also under development which should demonstrate that a balanced model is capable of handling the cooperative interaction of convective and balanced scales of motion implicitly.

The monotonicity principle underlying the existence of a unique element configuration cannot be applied if a mountain is 'grown' in the lower boundary since it can only be applied on either side of the mountain. (ie. M does not have to be monotonic on a curve such as the mountain surface). Nevertheless, it is still possible to compute a well-defined and physically meaningful set of equilibrium states in any problem involving flow over mountains. Consider the same initial data as that used in Fig. 6a but now with a rectangular block 'mountain' in the lower boundary. (Fig. 7a). Rather than introduce a uniform cross-mountain flow, we can equivalently move the mountain from right to left. Figs (7b,c) show successive equilibrium states. When an element interface rises up the windward face of the mountain to become tangential to the corner, the element involved splits into two. For instance, in Fig. 7(c) the boundary between elements 36 and 28 is tangential to the top left-hand corner of the mountain as fluid from element 36A jumps over the mountain and joins its other half (36B) which forms a shallow downstream 'dome'. The instantaneous transfer of mass between 36A and 36B can be thought of as a 'weir-like' geostrophic adjustment process. The potentially warm air on the lee-slope of the mountain block is to be contrasted with the cold air which 'dams up' on the windward side. It can be shown that this implies a pressure difference acting across the mountain equivalent to a stress of 8 Nm^{-2} acting over the horizontal area of the mountain. Pressure forces as

large as this are observed in the Swiss Alps during Föhn events (Hoinka, 1985) though they are difficult to reconcile with vertically propagating gravity wave momentum fluxes measured above. The model suggests that turbulent energy dissipation is probably taking place in the lee of the Alps associated with the sudden deceleration of the weir in a hydraulic jump. Further details can be found in Cullen, Chynoweth and Purser (1986).

3. Link with potential vorticity and the invertibility principle

When the fields $M(x,z)$ and $\theta(x,z)$ are continuous it can be shown that the Ertel potential vorticity q is proportional to the Jacobian of transformation, $J(\frac{M, \theta}{x, z})$ so that:

$$q \, dx \, dz \propto dM \, d\theta \quad (2)$$

Given a uniform discretization of data in (M, θ) space then (2) implies that the potential vorticity q_i of the i th element in our model is given by:

$$q_i \propto \frac{1}{A_i}$$

where A_i is the area of that element. (Note: a uniform discretization in (M, θ) space amounts to choosing a regular grid of points whose individual values correspond to element means in physical space). For example, a horizontally, stratified atmosphere composed of two regions of different static stability (troposphere and stratosphere) would have an element representation as in Fig. 8(a). Neighbouring layers of elements have potential temperature differing by a constant increment $\Delta\theta$ and neighbouring columns are different in M by a constant ΔM . The stratosphere is then manifest as a rectangular region composed of small elements ie. large q .

We consider now a complementary problem to the familiar elliptic invertibility problem discussed by Hoskins, McIntyre and Robertson (1985). Instead of specifying the distribution of q as a function of x and z

(together with appropriate boundary conditions) and solving for the pressure, we specify the area of elements with known M and θ and then determine the element geometry in physical space which gives the pressure field. No boundary conditions are applied in the latter dual space problem - at least not in the usual sense. All that is required is that elements fill the domain in physical space.

From the element configuration of Fig. 8(a) it is possible to produce a similar cut-off low cross-section to that given in Hoskins et al (1985) (their Fig. 15) by shrinking the area of elements just beneath the 'stratosphere' so as to create a tropopause funnel. This is equivalent to introducing a potential vorticity maximum into the two upper-most tropospheric layers. To maintain the same total element area, all other elements are expanded equally by the required fraction so that:

$$\sum_{i=1}^N A_i = \text{area of the domain}$$

Fig. 8(b) shows how the tropospheric isentropic layers are raised beneath the potential vorticity maximum and vice versa in the stratosphere. The associated v_g field is given in Fig 8(c) and shows the familiar equivalent barotropic structure of the cut-off low with peak winds at the tropopause.

4. Three-dimensional geometric models and their time integration

It can rigorously be shown that the monotonicity principle applies also in three-dimensional systems where the other absolute momentum component $N(=fy-u_g)$ is included. Now, M , N and θ must be monotonic along any straight line in the system such that M increases in the x -direction, N increases in the y -direction and θ increases in the z -direction. Again, a

modified pressure $P(x,y,z) = \phi + 1/2 f^2(x^2+y^2)$ forms the basis of the geometrical construction. Elements are now convex polyhedra and $P(x,y,z)$ is a piecewise linear function such that:

$$P(x,z) = \max_{j=1,N} \{ xM_j + yN_j + z\theta_j + s_j \}$$

The 'invertibility problem' of the last section has also been carried out in a 400 element three-dimensional model by shrinking a single element though the results are not shown here.

The evolution equations are simply those of semi-geostrophic theory and can be written as:

$$\frac{dM}{dt} = f (fy - N) \quad (3)$$

$$\frac{dN}{dt} = f (M - fx) \quad (4)$$

$$\text{and} \quad \frac{d\theta}{dt} = 0 \quad (5)$$

Eqs: (3-5) are ordinary differential equations governing the time evolution of M , N and θ for each element. In the incompressible system element volumes are preserved following the motion. After each time step the geometry is re-constructed using the new M , N and θ values. x and y for each element is then given by its new position.

At the time of writing our attempts to integrate these equations, for a two-dimensional barotropic problem (eqs. 3 and 4) using leap-frog methods, have failed. It is clear that implicit methods of time integration are needed such that x and y have 'future' information in them. A rather elaborate scheme has been developed and is to be tested shortly.

With the successful implementation of this scheme it should be possible to integrate the three-dimensional geometric model with the ultimate aim of examining a frictionless baroclinic wave life-cycle.

5. Potential advantages of the inviscid, Lagrangian model

A number of properties of this geometric model make it an extremely attractive tool for studying atmospheric dynamics and for providing 'prototype' solutions towards which finite-difference models should converge. They are:

- 1) The ability to handle discontinuities.
- 2) No eddy diffusion requirement.
- 3) Fluid can separate from boundaries (eg. the occlusion process)
- 4) The model automatically performs convective adjustments (eg. slantwise convection) at a rate controlled by the large-scale dynamical evolution.
- 5) In principal at least, mountain barrier effects (eg. drag) can be represented without parametrization.

Because discontinuities are a natural feature in a piecewise constant representation of meteorological fields, frontogenesis can proceed beyond the initial formation of boundary discontinuities (Hoskins and Bretherton, 1972). It is necessary to define what a discontinuity is in the element model since element boundaries are surfaces of discontinuity. We say that a discontinuity has formed when two elements, initially separated by a third element, make contact. For instance, in Fig. 4(b), a discontinuity in M exists between elements 29 and 31 after element 30 has convected to its new equilibrium level.

Allied to the ability to represent discontinuous structure is the option of omitting any sub-grid scale turbulence parametrization. Whilst such eddy diffusion terms are frequently rationalized as a physical representation of quasi-two-dimensional turbulence on sub-grid scales they are primarily a device for maintaining smooth fields and preventing computational noise. Although the eddy diffusion terms are typically small at any instant they may play an important role in the longer term energy and enstrophy budgets. For instance, in the baroclinic wave life cycle experiments of Simmons and Hoskins (1978), one half of the available potential energy decrease over the course of the experiment was dissipated rather than released as kinetic energy. All of this dissipation resulted from the internal diffusion terms since no boundary layer friction processes were included. Of course, it is reasonable to expect some turbulent energy dissipation to occur in frontal zones though at horizontal grid resolutions of ~ 150 km, it is bound to be excessive. Simmons and Hoskins calculated the hemispheric average of the energy dissipation rate during their life-cycle experiment. This peaked at a value of about 1 Wm^{-2} which is comparable with the energy dissipation rate, averaged throughout the depth of the Ekman boundary layer. Since frontal zones occupy only a small fraction of the area of the globe, the implied local energy dissipation rates in their model must be very much greater, (say a factor of 100). Energy dissipation rates measured during the Scillonia Project (eg. Roach and Hardman 1975) suggest substantially smaller values - more comparable with boundary layer dissipation than the rigorous turbulent mixing implied by sub-grid scale parametrization. Admittedly, dissipation rates measured in the warm front studied by Roach and Hardman may not be representative of frontal dissipation as a whole and further observational

work needs to be carried out. This could be an important scientific objective of the forthcoming European Frontal Dynamics Project. Because in principle, the geometric model is capable of integrating the semi-geostrophic equations without dissipation an inviscid life-cycle experiment could be simulated. Important differences between this proposed inviscid life-cycle and that of Simmons and Hoskins are implied by the radically different energetics.

Many circumstances exist in geophysical fluid dynamics for which fluid initially in contact with a boundary will tend to leave the boundary or separate. Fluid parcels themselves will, in certain circumstances, tend to flow past one another separated by an intense shear zone (or vortex sheet) as is commonly observed at the top of the convective boundary layer. Such processes require enormous resolution if they are to be realized at high Reynolds number with minimal spurious energy dissipation. Numerical weather prediction models with only a few 'levels' in the boundary layer have difficulty in separating air from the ground at surface cold fronts and the computational noise generated has to be controlled by internal friction.

In the oceanic context, the specification of lateral boundary conditions in ocean basin models depends on arbitrary choices of finite-difference scheme and frequently involves the concept of a coastal frictional boundary layer. Marshall (1982) has shown that in barotropic models the position at which boundary currents detach is a sensitive function of boundary conditions and finite-difference scheme. A barotropic version of the Geometric model would require no boundary conditions in the conventional sense - only the requirement that all elements fit into the domain. The surfacing of the main thermocline in a baroclinic ocean model

could be treated as an inviscid process in the geometric model and the point of Gulf stream detachment from the coast would not be influenced by frictional parametrization.

The ability of the Geometric model to maintain stability in a way consistent with the Lagrangian conservation laws removes the need for specific models of convection and its parametrization (eg moist convective adjustment). In general, the model's convective stabilization is a moist slantwise adjustment process involving no entrainment/mixing hypotheses. Since the geometric model only deals with sequences of quasi-equilibrium states, balanced energy (potential and kinetic) is lost after a convective 'jump' takes place. In strongly vertically-sheared flows, convection is often organised so as to inject released kinetic energy into the balanced flow through upgradient momentum transport (Moncrieff, 1978). Green, Ludlam and McIlveen (1966) argued that warm, moist boundary layer air may ascend in large-scale baroclinic waves to the upper troposphere and release kinetic energy into the jetstream consistent with a generalized Bernoulli theorem for steady flow (see also the correction pointed out by Betts (1969)). Ascent at cold fronts may involve slantwise convection organised in a similar way. If small-scale momentum transport is important then the Geometric model can easily accommodate this and would be tolerant of upgradient transport provided that it is energetically consistent.

The practical implementation of a three-dimensional Geometric model with mountains would be extremely difficult. Nevertheless, as the two-dimensional solutions described earlier show, important barrier and Foehn effects can be explicitly represented. Substantial mountain drag could be accrued from razor-thin mountain ridges - a contribution which would go unrepresented in a conventional finite-difference model where

mountain heights are based on grid-box volume averages. We believe that the difficulty underlying the representation of mountains in the Geometric model is symptomatic of the real nature of the problem rather than an unreasonable weakness of the element approach.

Our present philosophy is to regard the geometric model solutions as ideal, balanced solutions towards which finite-difference semi-geostrophic models should converge as resolution increases. Fully implicit finite-difference models have been built and are to be 'trained' to perform the inertial and convective stabilization that the geometric model does automatically. Some success in this direction has been achieved using a two-dimensional model.

Acknowledgements

Some of the geometric model calculations were carried out by Mr M Holt. We would also like to thank Dr S Clough for pointing out the work of Roach and Hardman.

References

- | | | |
|---|------|---|
| Betts, A.K. | 1969 | 'The energy formula in a moving reference frame'. Quart. J. Roy. Met. Soc., <u>95</u> , 639-642. |
| Cullen, M.J.P. | 1983 | 'Solutions to a model of a front forced by deformation'. Quart. J. Roy. Met. Soc., <u>109</u> , 565-573. |
| Cullen, M.J.P.,
Chynoweth, S.,
and Purser, R.J. | 1986 | 'On some aspects of flow over synoptic scale topography'. Quart. J. Roy. Met. Soc. (to appear). |
| Cullen, M.J.P.
and Purser, R.J. | 1984 | 'An extended Lagrangian theory of semi-geostrophic frontogenesis'. J. Atmos. Sci., <u>41</u> , 1477-1497. |

- Eliassen, A. 1948 'The quasi-static equations of motion'.
Geophys. Publ., 17, No. 3.
- Emanuel, K. 1983 'The Lagrangian parcel dynamics of moist
symmetric instability'. J. Atmos. Sci., 40,
2368-2376.
- Green, J.S.A.,
Ludlam, F.H. and
McIlveen, J.F.R. 1966 'Isentropic relative-flow analysis and the
parcel theory'. Quart. J. Roy. Met. Soc., 92,
210-219.
- Hoinka, K.P. 1985 'Observation of the airflow over the Alps
during a Foehn event'. Quart. J. Roy. Met.
Soc., 111, 199-224.
- Hoskins, B.J. 1972 'Atmospheric frontogenesis models: mathematical
and Bretherton, F.P. formulation and solution'. J. Atmos. Sci.,
29, 11-37.
- Hoskins, B.J., 1985 'On the use and significance of isentropic
McIntyre, M.E. potential vorticity maps'. Quart. J. Roy. Met.
and Robertson, A.W. Soc., 111, 877-946.
- Manabe, S. 1967 'Thermal equilibrium of the atmosphere with a
and Wetherald, R.T. given distribution of relative humidity'.
J. Atmos. Sci., 24, 241-259.
- Marshall, J.C. 1982 'Finite difference schemes and vorticity
boundary conditions in ocean models'.
(unpublished note).

- Moncrieff, M.W. 1978 'The dynamical structure of two-dimensional steady convection in constant shear'. Quart. J. Roy. Met. Soc., 98, 336-352.
- Roach, W.T. and 1975 'Mesoscale air motions derived from wind
Hardman, M.E. finding dropsonde data: the warm front and rainbands of 18 January 1971. Quart. J. Roy. Met. Soc., 101, 437-462.
- Simmons, A.J. 1978 'The life cycles of some non-linear baroclinic
and Hoskins, B.J. waves'. J. Atmos. Sci., 35, 414-432.

Figure Legends

1. Vertical column model of a convectively stable atmospheric profile i.e. potential temperature increasing with height.
2. One-dimensional barotropic atmosphere with inertial stability ie. absolute momentum increasing with x.
3. A three-element model of frontal occlusion.
 - (a) Before deformation.
 - (b) After deformation. (area scaled to be equal to (a)).

The absolute momenta and areas of the elements have been decreased in proportion to the total deformation.

- 4.(a) Initial element representation of stably-stratified atmosphere at rest.

(b) The equilibrium flow configuration after heat is added to element

30.

5. A sea-breeze front simulated by adding heat to the elements in contact with the 'land half' of the lower boundary.

6. (a) Initial element geometry corresponding to a cross-section through a front. Vertical (horizontal) element interfaces indicate elements having the same potential temperature (absolute momentum).

(b) Element geometry after the potential temperature of element 28 has been raised by 40°K.

7. (a) Initial element configuration for a model of flow over a rectangular block mountain (height 2 km).

(b) Element geometry six hours after (a) during which time the mountain is moved from right to left.

(c) Element geometry twelve hours after (a).

8. (a) Initial rest-state element geometry composed of a troposphere 10 km deep and a stratosphere 5 km deep. Neighbouring isentropic layers have a potential temperature differences of 8°K . Elements containing dots are to be shrunk.

(b) Element geometry after dotted elements have been reduced to the size of the stratospheric elements.

(c) Geostrophic velocity field V_g (into the picture) associated with (b).

Fig. 1

θ_5
θ_4
θ_3
θ_2
θ_1

$$\theta_{i+1} > \theta_i$$

$$i = 1, 4$$

Fig. 2

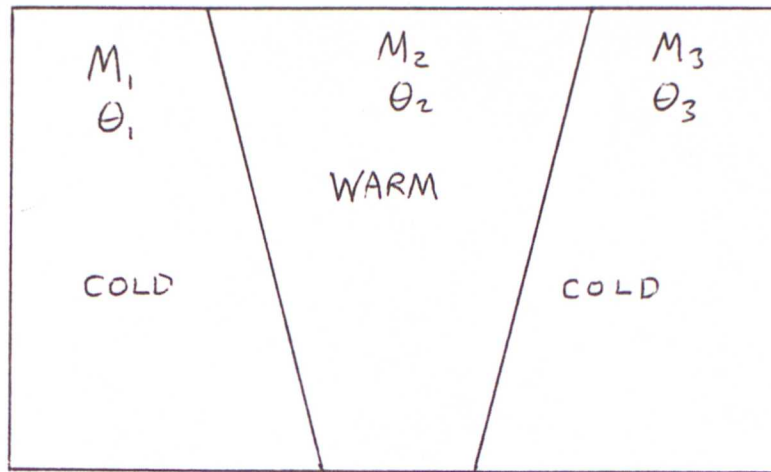
M_1	M_2	M_3	M_4	M_5
-------	-------	-------	-------	-------

$$M_{i+1} > M_i$$

$$i = 1, 4$$

Fig. 3

(a)



$$M_3 > M_2 > M_1$$

$$\theta_2 > \theta_1, \theta_3$$

(b)

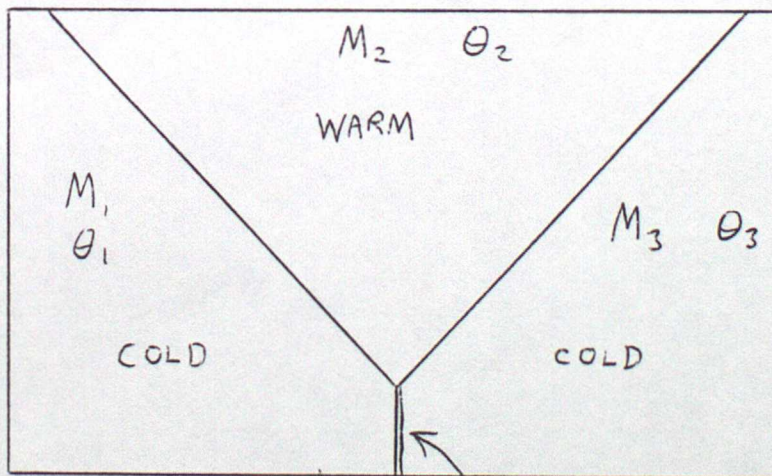


Fig. 4(a)

TIME STEP= 1 ISTEP= 5

81	82	83	84	85	86	87	88	89	90	91	92	93	94	95	96	97	98	99	100
61	62	63	64	65	66	67	68	69	70	71	72	73	74	75	76	77	78	79	80
41	42	43	44	45	46	47	48	49	50	51	52	53	54	55	56	57	58	59	60
21	22	23	24	25	26	27	28	29	30	31	32	33	34	35	36	37	38	39	40
1	2	3	4	5	6	7	8	9	10	11	12	13	14	15	16	17	18	19	20

Fig. 4(b)

TIME STEP= 10 ISTEP= 6

81	82	83	84	85	86	87	88	89	90	91	92	93	94	95	96	97	98	99	100
61	62	63	64	65	66	67	68	69	70	71	72	73	74	75	76	77	78	79	80
41	42	43	44	45	46	47	48	49	50	51	52	53	54	55	56	57	58	59	60
21	22	23	24	25	26	27	28	29	31	32	33	34	35	36	37	38	39	40	
		3	4	5	6	7	8	9	10	11	12	13	14	15	16	17	18	19	20

4 km

SEA-BREEZE MODEL

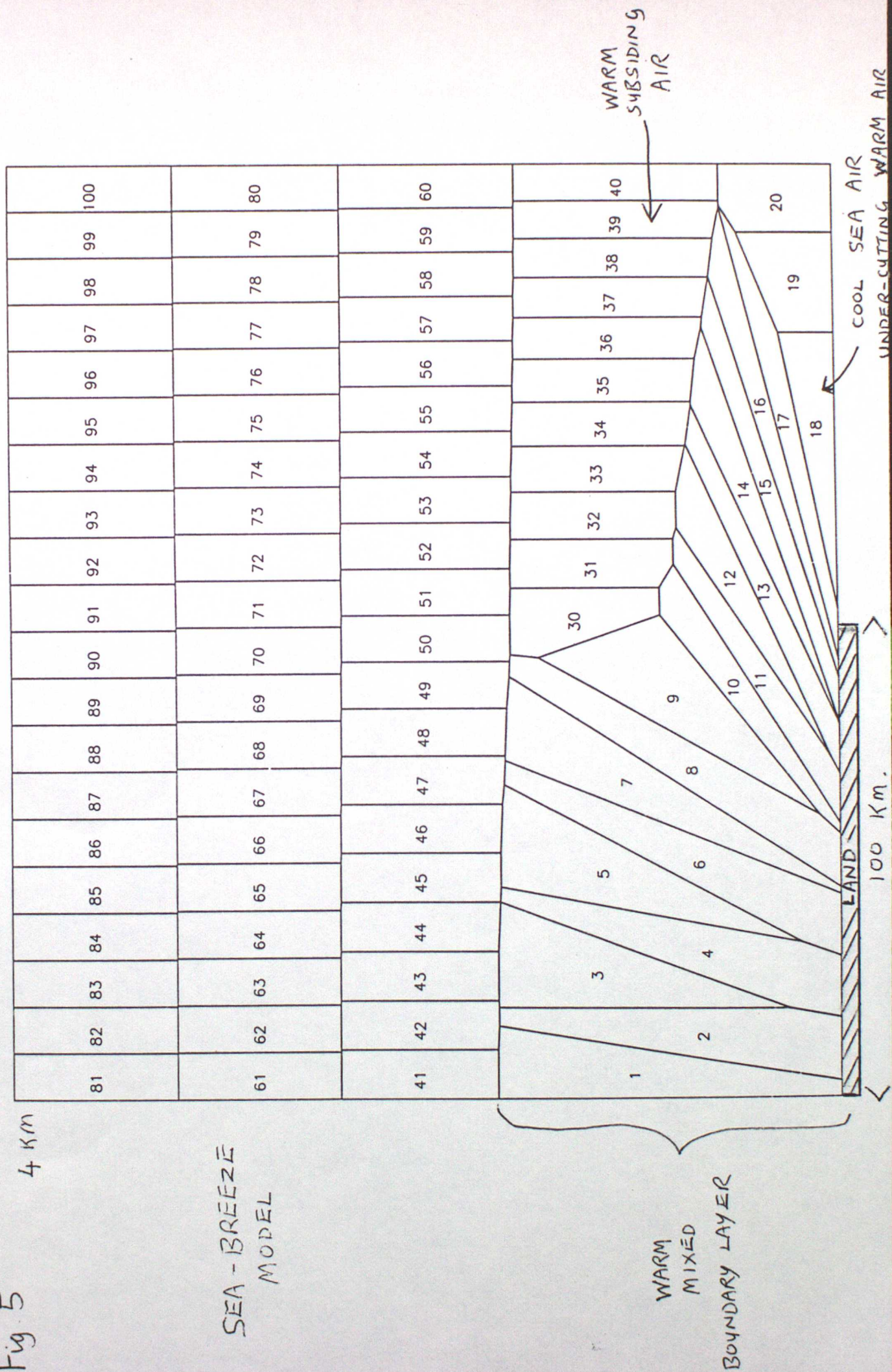


Fig. 6(a)

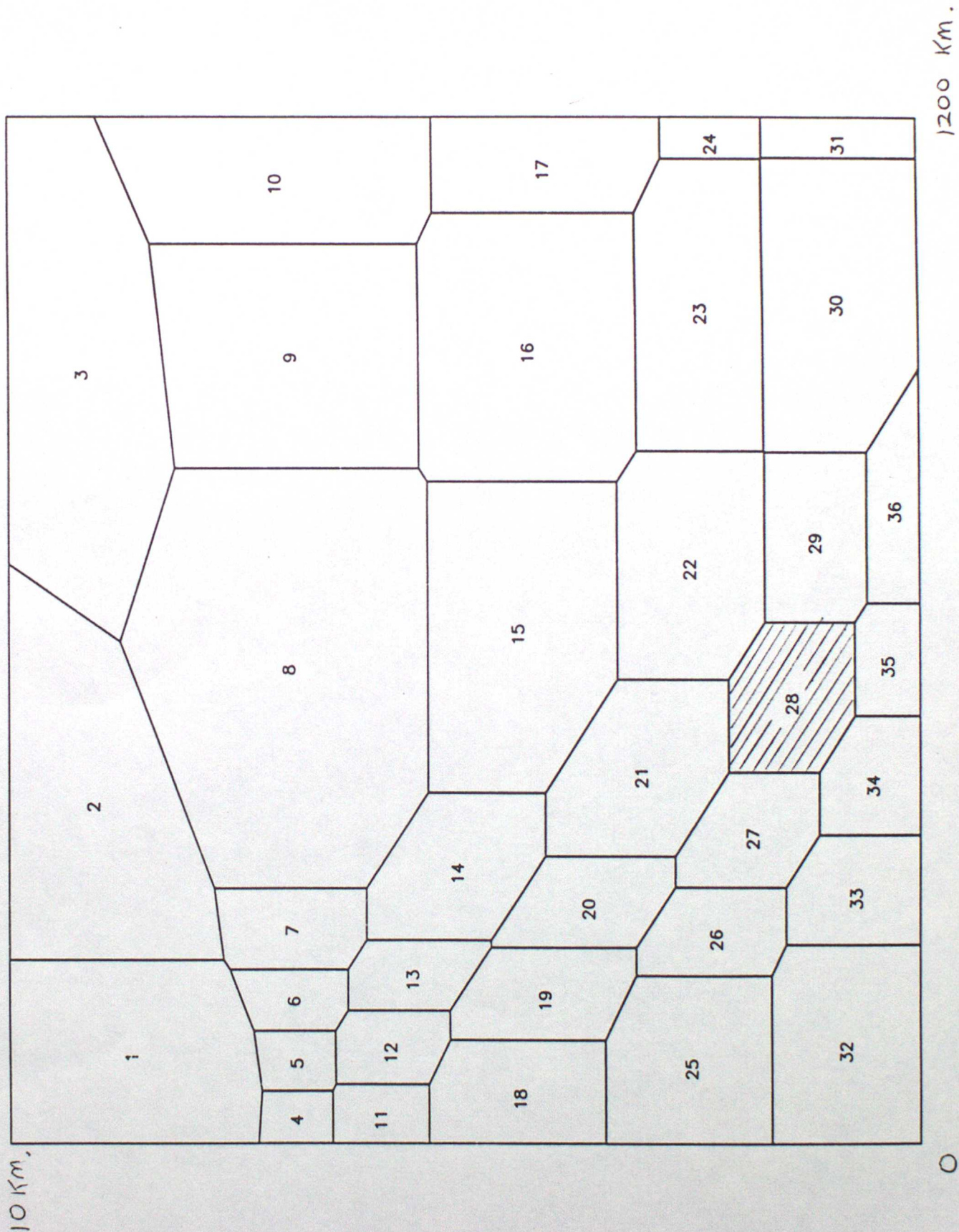


Fig. 6 (b)

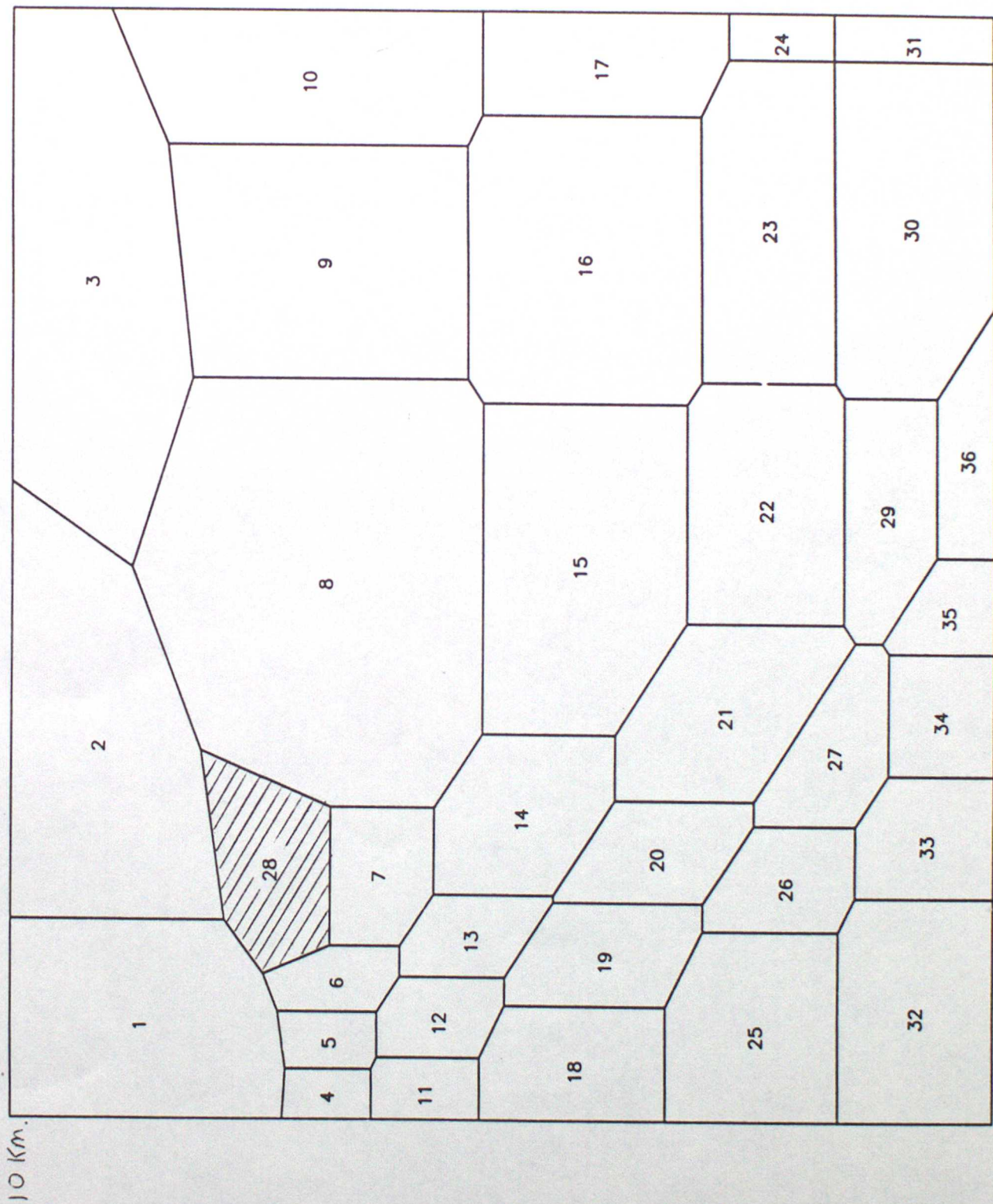


Fig. 7 (a)

INITIAL DISTRIBUTION OF FLUID ELEMENTS (2/4/73 12Z)

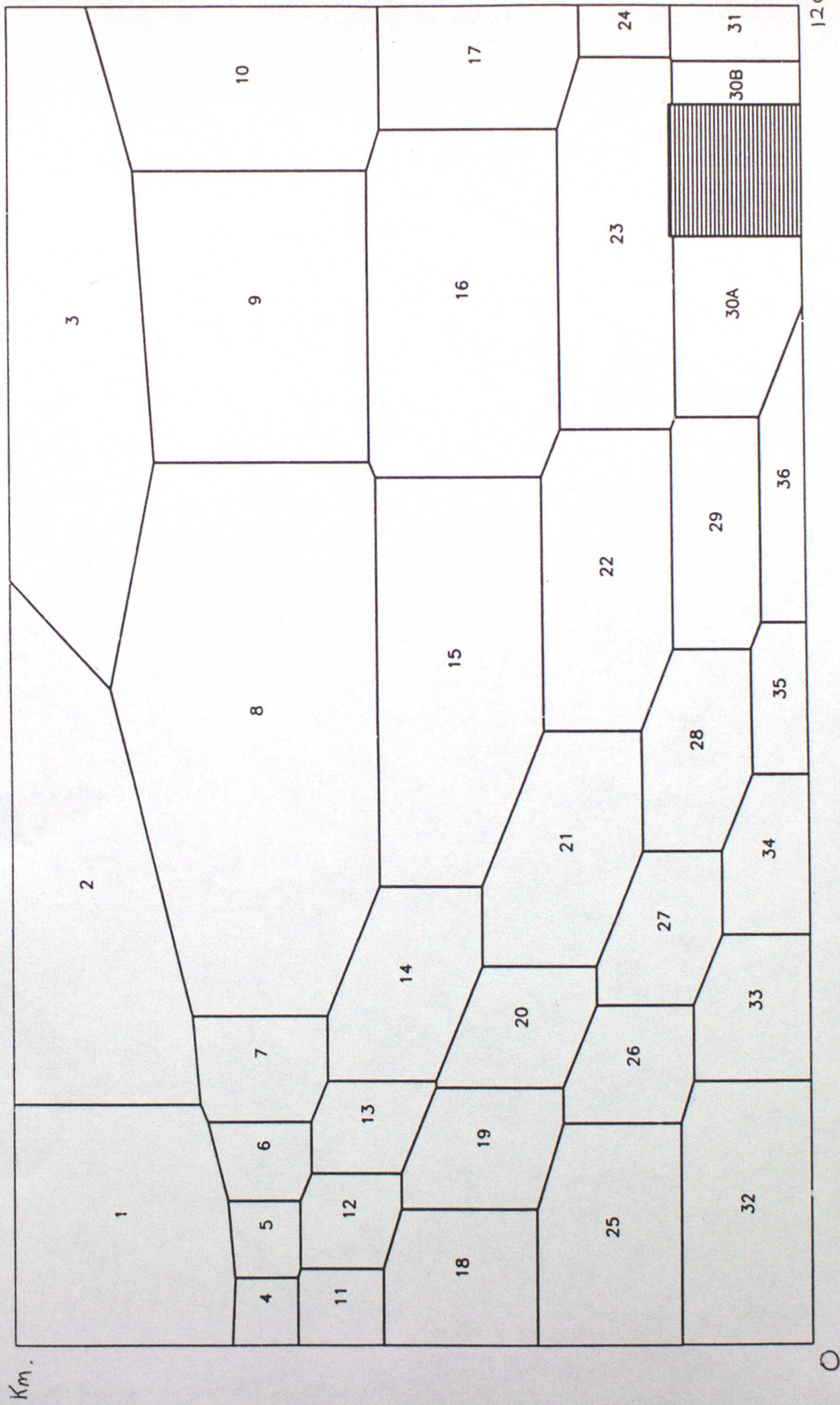


Fig 7(b)

DISTRIBUTION OF FLUID ELEMENTS AFTER SIX HOURS (2/4/73 18Z)

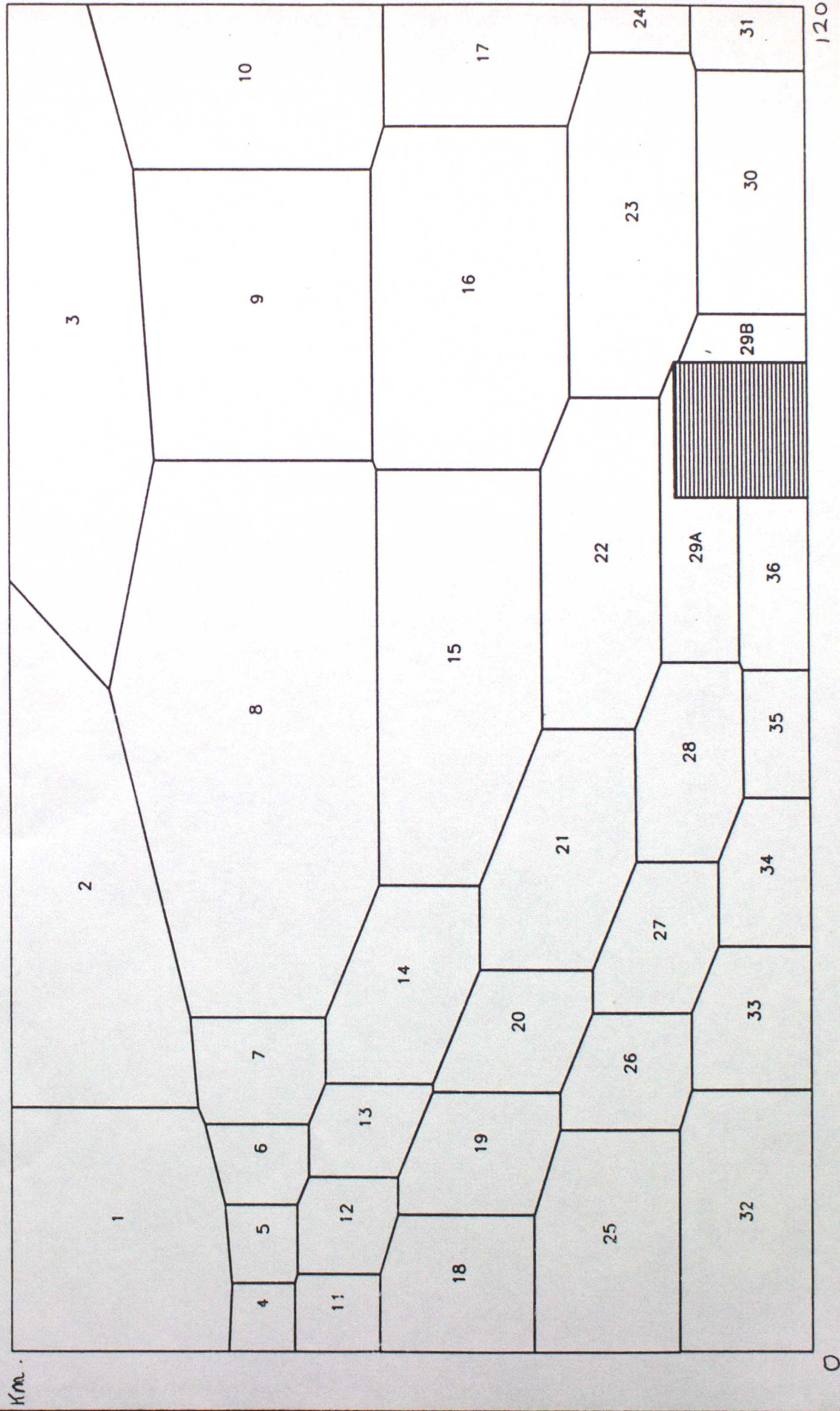


Fig. 8 (a)

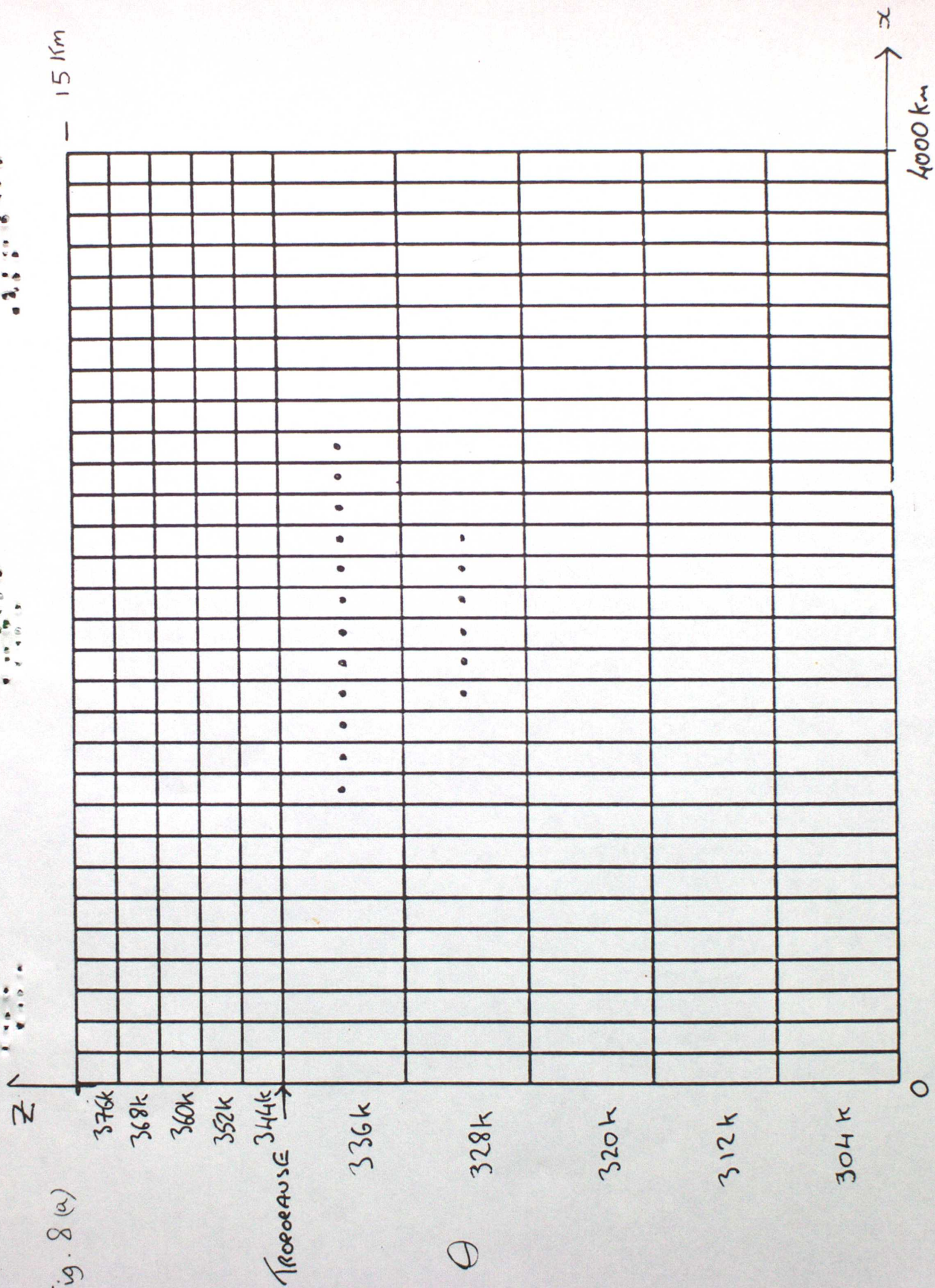


Fig. 8 (b)

- 15 km:

